MDPI

Article

Effect of Thermal Management Approaches on Geometry and Productivity of Thin-Walled Structures of ER 5356 Built by Wire + Arc Additive Manufacturing

Leandro João da Silva [1,*], Henrique Nardon Ferraresi [1], Douglas Bezerra Araújo [1], Ruham Pablo Reis [1] and Américo Scotti [1,2]

1   Center for Research and Development of Welding Processes (Laprosolda),
    Department of Mechanical Engineering, Federal University of Uberlandia (UFU),
    Uberlândia 38408-100, Brazil; henriquenardon@gmail.com (H.N.F.); dbaraujo@ufu.br (D.B.A.);
    ruhamreis@ufu.br (R.P.R.); americo.scotti@hv.se (A.S.)
2   Division of Welding Technology, Production Technology West, Department of Engineering Science,
    University West, 461 32 Trollhättan, Sweden
*   Correspondence: leandro.js@ufu.br

Abstract: The present paper aimed at assessing the effect of two thermal management approaches on geometry and productivity of thin-walled structures built by Wire + Arc Additive Manufacturing (WAAM). Thin-walls of ER 5356 (Al5Mg) with different lengths and the same number of layers were deposited via the gas metal arc (GMA) process with the aid of an active cooling technique (near-immersion active cooling—NIAC) under a fixed set of deposition parameters. Then, the same experiment was performed with natural cooling (NC) in air. To characterize the thermal management approaches, the interpass temperature (i.e., the temperature at which subsequent layers are deposited) were monitored by a trailing/leading infrared pyrometer during the deposition time. Finally, thin walls with a fixed length were deposited using the NC and NIAC approaches with equivalent interpass temperatures. As expected, the shorter the wall length the more intense the deposition concentration, heat accumulation, and, thus, geometric deviation. This behavior was more evident and premature for the NC strategy due to its lower heat sinking effectiveness. The main finding was that, regardless of the thermal management technique applied, if the same interpass temperature is selected and maintained, the geometry of the part being built tends to be stable and very similar. However, the total deposition time is somewhat shorter with the NIAC technique due its greater heat sinking advantage. Thus, the NIAC technique facilitates the non-stop manufacturing of small parts and details via WAAM.

Keywords: directed energy deposition; wire + arc additive manufacturing; cold metal transfer; thin-walled structures; thermal management; part geometry; production time

1. Introduction

The ASTM F3187 [1] standard guide for directed energy deposition (DED) of metals states that preheating temperature and interpass temperature may be key variables for certain processes and materials. This is particularly true for the fabrication of thin-walled structures by Wire + Arc Additive Manufacturing (WAAM) due to its high deposition rate/heat input and a poor heat sinking effect through thin-walled structures.

In welding technology [2], preheating is the temperature to which the surfaces to be welded together are heated before welding, and interpass temperature is the temperature at which subsequent weld runs are executed. In welding, minimum interpass temperatures are maintained to control the microstructure produced, and, in most cases, they are similar to the preheating temperature. Similar concepts can be translated to WAAM. However, in addition to the microstructure, the interpass temperature has a significant effect on the part

geometry [3]. It is worth mentioning that a layer may be formed of various passes and, therefore, the term "interlayer temperature" is also found in the literature. In the case of thin-walled structures, which generally consist of one pass per layer, both terminologies could be used.

Thermal management can be defined as a set of approaches and techniques used to control the temperature (by heating or cooling) of the part during the entire deposition time (sometimes not) and in some cases thereafter. Since geometries are typically more complex in WAAM parts than in welded ones, the challenge involving temperature control begins at how and where to measure the interpass temperature. Wu et al. [4] explain that if the temperature measured at a substrate is taken to be the interpass temperature it will cause large errors. Hagqvist et al. [5] argue that the measuring of interpass temperature with a thermocouple is impractical due to DED's layer by layer nature. Both authors agree that the measurement of current layer temperature with non-contact infrared (IR) pyrometer provides far more accurate data.

The lack of proper thermal management can lead to heat accumulation [6]. In practice, heat accumulation is characterized by the consecutive increase in the part temperature during the manufacturing time [6]. In an extreme case, the heat accumulation can lead to the part's collapse [7], but before that it can cause problems of a metallurgical nature [8], geometric deviation [4], and excessive surface oxidation [9].

Among the many advantages reported in the current literature, the WAAM process is referred to as being suitable for the deposition of large metallic components, typically heavier than 10 kg [10]. However, even large components may have minor localized features, such as the nose cone and fins (short isolated walls) in the rocket-shaped preform shown in Figure 1, which could lead to deposition concentration and, without appropriate thermal management, to localized heat accumulation.

Figure 1. Thin-walled part of ER-5356 continuously deposited by WAAM with proper thermal management (Near-immersion Active Cooling technique as developed by da Silva et al. [6]) during preliminary tests (the continuous deposition, especially of the nose cone, would not be possible without proper thermal management due to the intense deposition concentration and consequent heat accumulation).

The heat accumulation issues are not new, but, currently, due to the notable academic and industrial interest in WAAM, different thermal management approaches have been proposed and implemented as summarized in Table 1.

Table 1. Some typical thermal management approaches for WAAM reported in the recent literature and their selected highlights.

Reference	Thermal Management Approach	Deposition Process and Material	Selected Highlights
[8]	In-process cooling with liquid N_2 (cryogenic)	GMA [1] and AISI 316L	In-process cooling promoted grain refinement and improvement of mechanical properties.
[11]	Dwell time (natural cooling)	GMA and low carbon steel	No heat accumulation occurred for interpass times above 5 min.
[12]	Cooling of the platform/substrate	GMA and low carbon steel	Thin walls were more difficult to deposit continuously without a compulsory cooling solution, i.e., natural condition.
[13]	Reduction of the deposition current	GTA [2] and Al-Si alloy	Reduction in deposition current (from 140 to 100 A over 40 layers) was sufficient to deal with heat accumulation.
[14]	Increasing of the travel speed	GMA and low carbon steel	Layer width was kept constant along the part cross section by increasing the welding speed as the layers were deposited.
[15]	Interpass cooling with compressed CO_2 jet	GTA and Ti6Al4V	Interpass cooling reduced oxidation and significantly increased productivity.
[16]	In-process cooling with compressed CO_2, N_2 and air	GMA and low carbon steel	CO_2 had better cooling effect than N_2, which exceeded the capacity of air.
[17]	Active cooling and variable polarity deposition current	GMA and Al-Mg alloy	Active cooling and deposition process approaches were used to mitigate heat accumulation, but the former was shown to be more efficient.
[18]	Active cooling and variable polarity deposition current	GMA and Al-Mg alloy	Active cooling and deposition process approaches affected macro and microstructural aspects of Al parts.

Plasma arc deposition processes acronyms are in concordance with ASTM 3187 guide [1], where: [1] GMA = gas metal arc. [2] GTA = gas tungsten arc.

The dwell/cooling time, hereinafter referred to as natural cooling (NC), is probably the most used thermal management approach. This is mainly because it does not require any new system to be implemented in the additive manufacturing machine. Despite the fact that the NC approach fulfils the objective of controlling the interpass temperature [11], it can prohibitively increase the deposition time. It may be more efficient than NC to execute the deposition on a cooled platform/substrate [11]. However, it is expected that its heat sinking power decreases as the part height increases, particularly for materials with low thermal diffusivity, such as austenitic stainless steels or nickel-based alloys. In general, parameter modulation [12,13] aims at reducing the heat input along with the deposition time. This approach has revealed excellent results as reviewed by Rosli et al. [19], whereas it implies reducing the deposition rate or the layer height for a processes with consumable electrodes, such as GMA. Forced convection with gases [15] is a solution for materials with low thermal diffusivity. However, to be efficient, it must be applied as close to the heat source as possible (before it diffuses through the part), which significantly increases the chance of arc disturbance. The Near-immersion Active Cooling (NIAC) technique, in which the part is produced inside a work tank that is filled with water as the layers are deposited [17], has been demonstrated to be capable of coping with heat accumulation. Nonetheless, its application might be restricted by a few issues—the water tank can be difficult to handle, especially in multi-axis manufacturing systems with a moving worktable [6].

In light of what has been examined so far concerning thermal management, it can be said that there are several approaches available to conduct it for DED processes, each option with its own advantages and limitations. The main challenge that remains is implementing an approach applicable to most geometries without jeopardizing productivity and even allowing its improvement. Therefore, the present paper aims at assessing the effect of NC and active cooling (NIAC) thermal management approaches on the geometry

and productivity of thin-walled structures built by WAAM with ER 5356 (Al5Mg) wire. Although the present work has been focused on thin-walled structures of an ordinary Al5Mg alloy produced by WAAM with NC and NIAC thermal managements, the results can be translated for other DED processes, thermal management techniques, and materials.

2. Materials and Methods

Thin-walled structures were deposited in the NIAC rig developed by da Silva [20] (Laprosolda, Uberlândia, Brazil). The same rig was used for the NC experiments. The depositions were carried out on vertical clamped substrates to mimic wall-like preforms in terms of heat flux and stiffness since the beginning. Deposition conditions are summarized in Table 2.

Table 2. Deposition conditions.

Arc Deposition Equipment	Fronius CMT—TransPuls Synergic 5000
Wire (deposition material)	AWS ER 5356—Ø 1.0 mm
Shielding gas	Commercially pure argon at 12 L/min
Synergic line code	CMT 1070
Substrate	Al5052 (330 mm × 38.1 mm × 6.35 mm)
Wire feed speed [1]	7.6 m/min
Arc current [1]	96 A
Arc voltage [1]	8.5 V
Deposition speed	60 cm/min
Arc energy	82 J/mm
CTWD [2]	12 mm
LEWD [3]	5, 10, 15, and 30 mm
Cooling liquid	Tap water
Work tank volume	50 L
Preform geometry	Single wall with 20 layers
Preform lengths	100, 1500, 200, 250, 300 and 350 mm
Building strategy	Single-pass multi-layer bidirectional depositions
Dwell time	5 s/layer

[1] Measured average values. [2] CTWD = contact tube to work distance. [3] LEWD = layer edge to water distance.

Figure 2 shows the infrared (IR) pyrometer (Advanced Energy, Fort Collins, Colorado, USA) arrangement employed for in-processing-measuring of the interpass temperature in the layer surface. Data from a 0.6 mm diameter (each wire) K-type thermocouple was used to adjust the pyrometer emissivity to 22%. The pyrometer measuring spot target was kept close but at 30 mm from the arc center, since the signal got very noisy for shorter distances. The pyrometer specification is in Table 3.
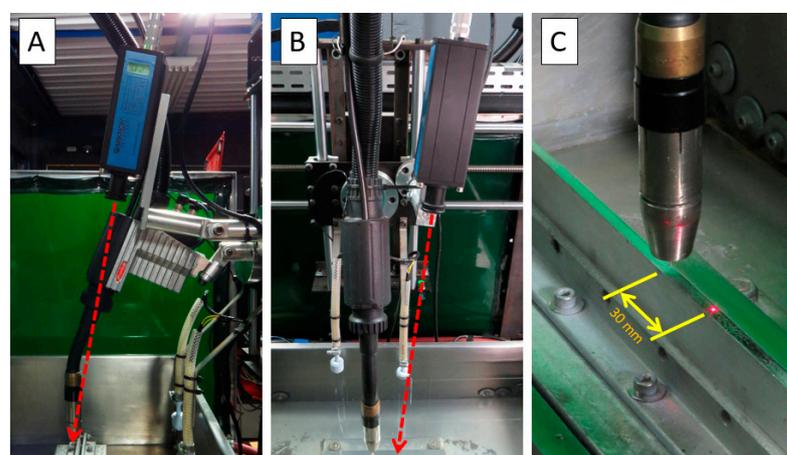

Figure 2. IR pyrometer arrangement for in-processing-measuring of the interpass temperature: (**A**) front view; (**B**) lateral view; (**C**) measuring spot target.
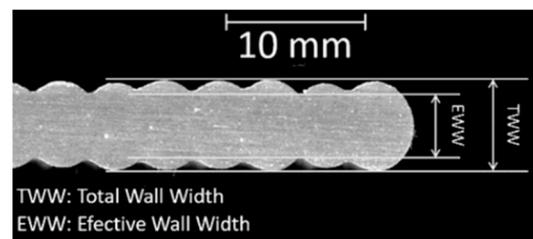
Table 3. IR pyrometer specification.

IR Pyrometer	Mikron MI-PE140 with Focusable Optics
Spectral range	3–5 μm
Temperature range	30–1000 °C
Spot size	Ø 2.9 mm at 380 mm
Resolution	0.1 °C

The porosity level was estimated by the Archimedes method. In this case, a digital balance with a resolution of 0.01 g and distilled water were used. The preforms were cut from the substrate in samples of around 100 g. The porosity was then estimated from the density of a reasonable sample (100 g) of the Al wire used, which was calculated by using the same method. Three measurements were performed for each sample, both in the air and in the water. The results are presented in terms of volume of voids, since eventual internal cracks and/or lack of fusion defects may also affect the porosity results.

Geometrical features of the preforms, specifically the total wall width (TWW), effective wall width (EWW), and surface waviness (SW), were estimated from cross-sectional image analyses. All samples for this analysis were taken from the walls at their mid-length by abrasive cooled cutting and the respective surfaces were prepared by standard grinding with SiC sandpaper (320, 600, and 1200 mesh). Geometrical analyses were performed according to Martina et al.'s [21] definitions and da Silva et al.'s [20] approaches. For a better understanding, these features are illustrated in Figure 3 and calculated with Equation (1).

$$SW = \frac{TWW - EWW}{2} \tag{1}$$

Figure 3. Geometrical features measured to characterize the surface texture of the walls [20].

3. Results and Discussion

As expected, the LEWD (layer edge to water distance) parameter of the NIAC technique influences the visual and geometric aspect of the walls. As shown in Figure 4, for lower LEWD values (water closer to the deposition level) the lateral surface waviness tends to be higher and the top surface more undulated. For the NC condition, the surface of the walls got rougher and assumed a matte aspect, which may be related to the heat accumulation and/or to an insufficient shielding gas protection [20].

As the cross-sectional views, shown in Figure 5, were virtually constant along the wall length for all conditions, they can be considered representative of the entire length of each wall. The walls deposited under the NIAC technique were taller and slender than those ones produced under the NC approach. Also, it can be observed that the walls were more irregular and tended to become wider along the height under the NC approach. This behavior might be related to molten pool enlargement due to heat accumulation. Regardless of the surface waviness, the width of the walls deposited with the NIAC technique was almost constant along their heights (parallel lateral surfaces).
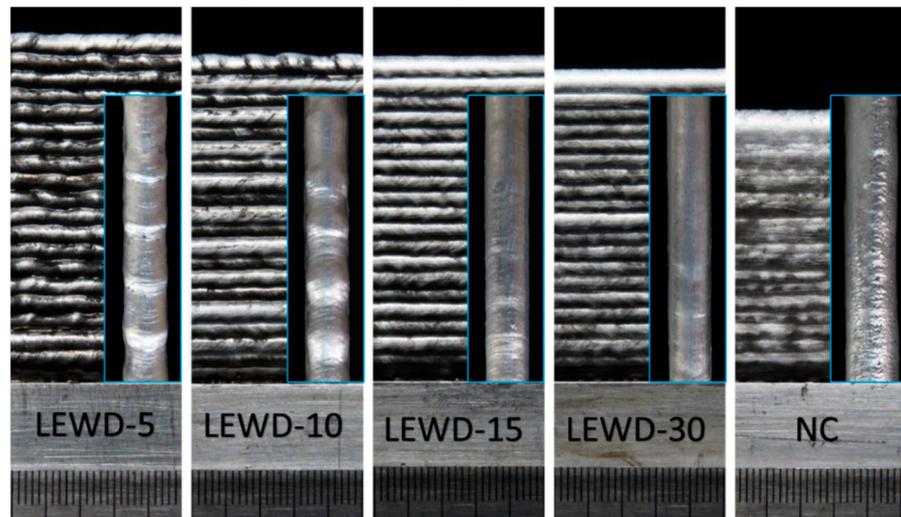
Figure 4. Effect of the LEWD parameter on the lateral and top superficial aspects of the 350 mm-long walls.
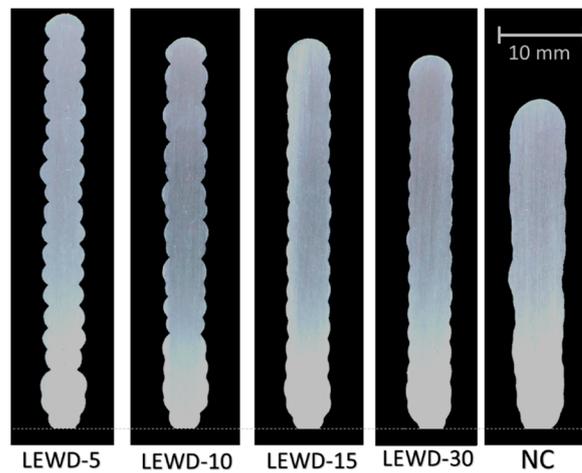

Figure 5. Qualitative effect of the LEWD parameter on the geometrical quality of the 350 mm-long walls.

As shown in Figure 6, the variation in the LEWD value had no significant effect on the TWW results (external width), but the EWW values increased with increasing LEWD values. This fact suggests that the higher the LEWD value (the weaker the heat sinking effect), the greater the volume of the anterior layer that is remelted. This suggestion agrees with the analytical model proposed by Ríos et al. [22], which predicts that the resultant SW depends on the remelted volume in an indirect proportional relationship. The relationship between the SW result and the LEWD value has a minimum for a LEWD between 15 and 30 mm. This minimum value of SW is in accordance with that reported in the current literature, as by Williams et al. [10].
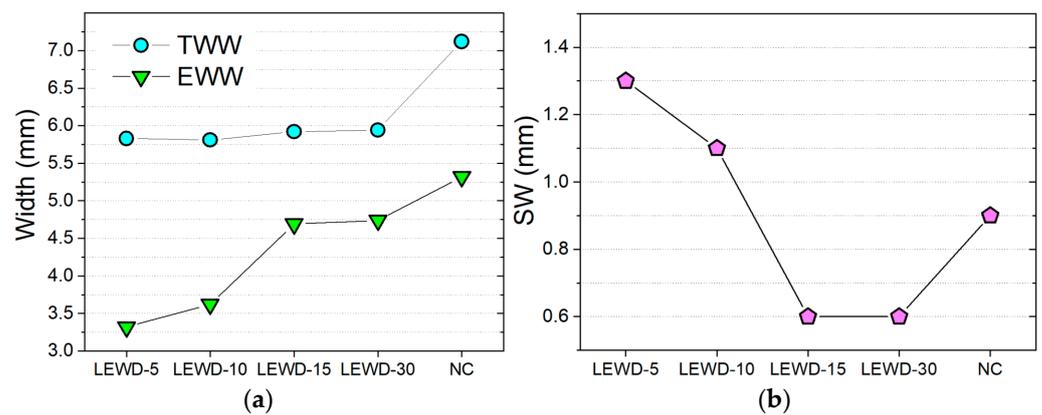
Figure 6. Quantitative effect of the LEWD parameter on the geometrical quality of the 350 mm-long walls: (**a**) effect of LEWD on the total and effective wall width and (**b**) on surface waviness.

In general, the porosity level of the walls was in accordance with previous exploration of the NIAC technique [20] and with the range commonly reported in the current literature [23]. As shown in Figure 7, the significant higher porosity level for the lowest LEWD value can be attributed to more intense water evaporation, which could hydrate the fresh oxides and/or contaminate the molten pool. There was also a tendency of porosity increase in the walls deposited under the NC approach. This behavior might be related to larger molten pool volumes in this case, which could absorb higher amounts of hydrogen [24], and/or due to heat cumulation, which may promote an intra-pore coalescence phenomenon and an expansion of trapped gas inside the pores [25,26].
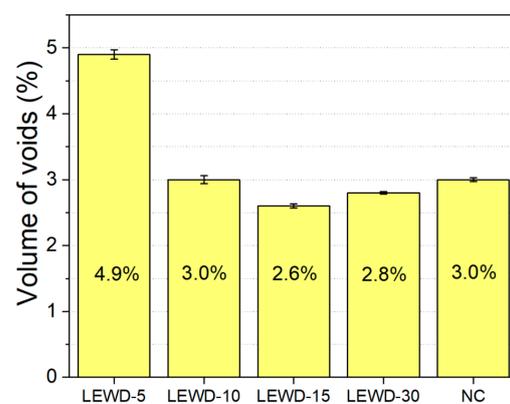

Figure 7. Effect of the LEWD parameter on the volume of voids of the 350 mm-long walls.

Because of the bidirectional deposition strategy, two levels of temperature can be distinguished, as shown in Figure 8 (one with pyrometer leading and another with it trailing the arc). The high level is the temperature of the newly-deposited layer measured at 30 mm behind the arc center. The low level represents the temperature measured at 30 mm ahead of the arc center, that is, measured in the previous lawyer. For the NC approach, both these levels are notably higher. In contrast, for the NIAC technique, the lower the LEWD value, the lower the levels of these temperatures due to the greater heat sinking effect. Also, it is possible to notice that there is a time for the temperature to stabilize, which depends on the thermal management technique applied (in some cases, for the deposition conditions employed, the walls were not long enough to reach the stabilization). Under the NIAC technique, the lower the LEWD value, the faster the temperature reaches a steady-state regime due to the higher heat sinking effect.
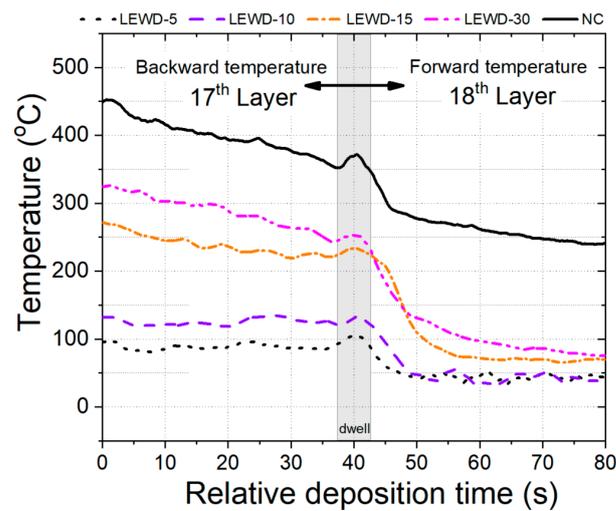
Figure 8. Temperature data from the trailing/leading IR pyrometer (after the deposition of 2 layers) of the 350 mm-long walls.

As shown in Figure 9, taking the NC approach as an example, the temperature data acquired from the trailing/leading IR pyrometer during all the deposition time (20 layers) tend to fit a bimodal distribution. The average temperature measured ahead of the arc (forward temperature—FT) corresponds to the first quartile Q1 (25%) and seems to be representative of the average interpass temperature. The temperature measured behind the arc (backward temperature—BT) corresponds to the third quartile Q3 (75%) and represents the average temperature of the ongoing layer at 30 mm behind the arc center. Hereinafter, to facilitate the comparison between different groups of data in terms of their quartiles, the temperature data from the trailing/leading IR pyrometer are represented through the boxplot method.
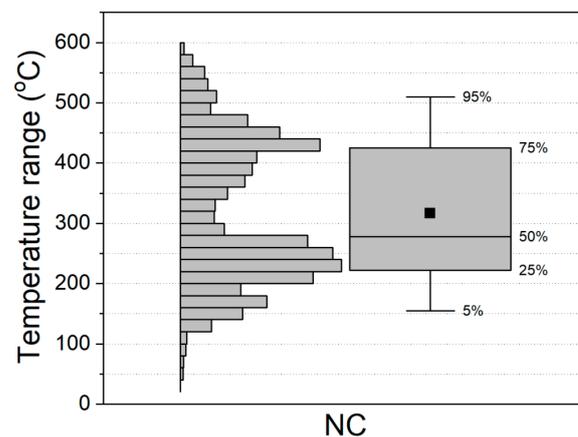

Figure 9. Temperature distribution based on the data acquired from the trailing/leading IR pyrometer during all the deposition time of a 300 mm-long wall with NC approached.

Figure 10 shows the effect of the LEWD parameter on the temperature data distribution, while Table 4 lists the values of the BT and FT results. The FT (25%) as well as the BT (75%) values tend to become lower as the LEWD value is reduced. However, the BT (the top line of the box) value is more sensible to the LEWD parameter variation than the FT (the bottom line of the box) one. The FT value appears to be more dependent on the water temperature than on the LEWD value used. Moreover, the interquartile range (Q3-Q1: the box height) is remarkably narrower with low LEWD values due to the correspondent larger heat sinking intensities. Therefore, for a low Q1 (interpass temperature) level, it sounds quite reasonable to link a low interquartile range to a high cooling rate of the layers.

This data can be used to control and even modify the microstructure of a given component throughout its volume, opening a wide window of opportunities.
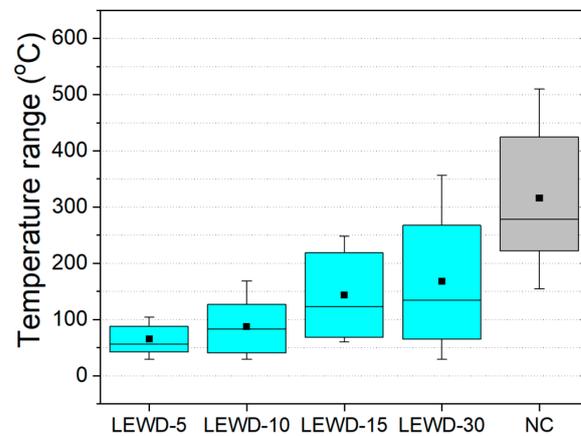

Figure 10. Effect of the LEWD parameter on the thermal features measured with the trailing/leading IR pyrometer in the 350 mm-long walls.

Table 4. Effect of the LEWD parameter on the average forward and backward temperatures of the 350 mm-long walls.

Layer Temperature	LEWD-5	LEWD-10	LEWD-15	LEWD-30	Natural
Forward temperature—FT (°C)	42	40	68	65	222
Backward temperature—BT (°C)	88	127	219	267	425

To analyze whether the FT (the bottom line of de boxplot: 25%) value is truly representative of the interpass temperature or not, a wall was deposited under the NC approach using the FT level as the criterion to resume the deposition of each new layer, i.e., in between each layer an interpass dwell time was added to allow air cooling until the FT reached a specific and fixed value. The cross-sectional views presented in Figure 11 show that the NC approach with an interpass temperature (measured at half-length) equivalent to the FT level achieved under the NIAC technique with the LEWD at 15 mm produced fairly similar walls. However, due to the dwell time demanded when using the NC strategy, the deposition in this case was significantly longer (49 min) than that with the NIAC technique (7 min). Moreover, it is also important to keep in mind that, despite being able to reach an equivalent geometry, the NC approach does not eliminate probable deleterious consequences of long exposures to high temperatures.

A set of experiments were executed to evaluate the NIAC technique performance in terms of conditions with deposition concentration, such as the example shown in Figure 1. To mimic different levels of deposition concentration, walls with different lengths were deposited with the NIAC and NC approaches. The deposition parameters, the LEWD value (15 mm) for the NIAC and the total number of layers (20) were kept constant. For the NC condition, as clearly seen in the cross-sectional views presented in Figure 12, the shorter the wall length, the more prominent the heat accumulation deleterious effect on the resultant geometry. The temperature data distribution shown in Figure 13 confirms that the more deposition concentration exists the hotter the preform. For walls shorter than 100 mm, the molten pool tends to collapse due to its very large volume as the wall height (number of layers) grow. As the length of the walls is increased, they become taller and slender because of the longer deposition times and, consequently, of the longer cooling times until the depositions are finished. It might be expected that above a certain length the deposition time of one layer will be long enough to suppress the heat accumulation.
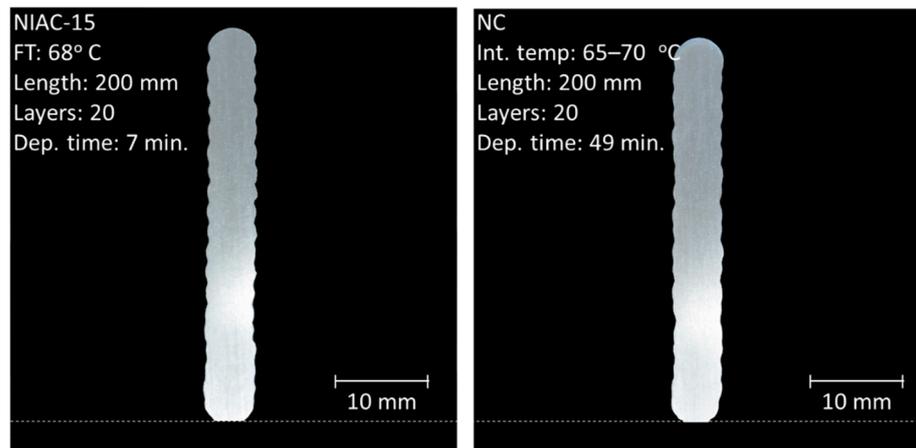
Figure 11. Comparison between 200 mm-long walls deposited with the NIAC and the NC approaches under equivalent interpass temperatures.
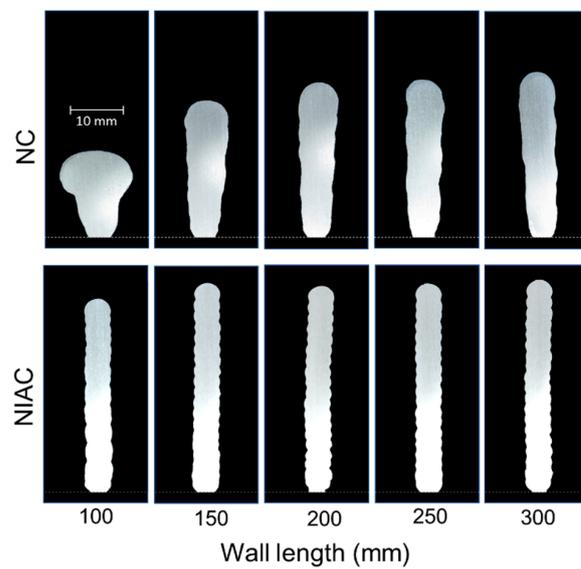

Figure 12. Effect of the deposition concentration on the geometry of walls with different lengths deposited with the NIAC (LEWD at 15 mm) and NC approaches.
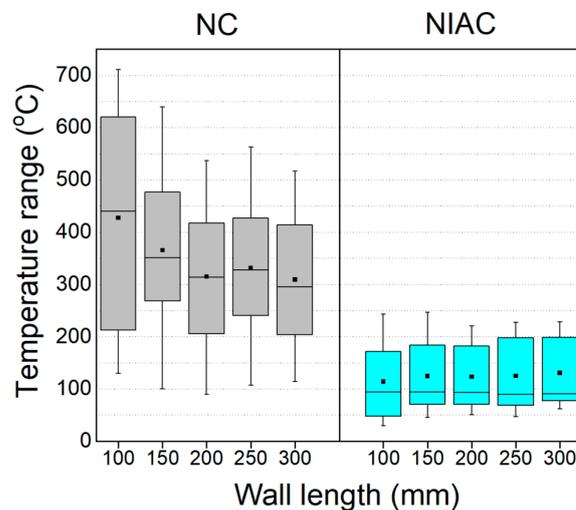

Figure 13. Comparison between temperature data distributions of walls built with different lengths under the NIAC (LEWD at 15 mm) and NC approaches.

4. Conclusions

The present paper aimed at assessing the effect of the near-immersion active cooling (NIAC) and natural cooling (NC) thermal management approaches on the geometry and productivity of thin-walled structures of ER 5356 (Al5Mg) built by Wire + Arc Additive Manufacturing (WAAM). From the results of such an investigation, the following conclusions can be drawn:

- The LEWD variation had no significant effect on the total width of the walls, while their effective width values increased and surface waviness levels reduced with increasing LEWD values;
- In general, the porosity level was in accordance with the numbers reported in the current literature, despite the fact it tends to significantly increase with LEWD values below 10 mm;
- In terms of geometry and porosity, the walls deposited under the NIAC technique with LEWD values between 15 and 20 mm showed more adequate results for the arc energy level (82 J/mm) and material (ER 5356) employed;
- The temperature data from the trailing/leading IR pyrometer extracted during the deposition time tend to fit a bimodal distribution, being the first quartile (Q1) representative of the interpass temperature;
- Thin-walled structures built with the NIAC and NC approaches can assume quite similar geometries if equivalent interpass temperatures are applied, but the total deposition time with the latter approach is significantly extended due to the need for long interpass dwell time;
- The NIAC technique has been demonstrated as able to cope with the heat accumulation due to deposition concentration, and being capable of aiding continuous building of small components and/or features by WAAM.

References

1. ASTM. *ASTM F3187-16-Standard Guide for Directed Energy Deposition of Metals*; ASTM International: West Conshohocken, PA, USA, 2016; pp. 1–22. [CrossRef]
2. TWI. Which is Important—Preheat or Interpass? Frequently Asked Questions. 2021. Available online: https://www.twi-global.com/technical-knowledge/faqs/faq-which-is-important-preheat-or-interpass (accessed on 23 August 2021).
3. da Silva, L.J.; Reis, R.P.; Scotti, A. The potential of IR pyrometry for monitoring interpass temperature in wire + arc additive manufacturing. *Evol. Mech. Eng.* **2019**, *3*, 1–4. [CrossRef]
4. Wu, B.; Ding, D.; Pan, Z.; Cuiuri, D.; Li, H.; Han, J.; Fei, Z. Effects of heat accumulation on the arc characteristics and metal transfer behavior in wire arc additive manufacturing of Ti6Al4V. *J. Mater. Process. Technol.* **2017**, *250*, 304–312. [CrossRef]
5. Hagqvist, P.; Sikström, F.; Christiansson, A.-K. Emissivity estimation for high temperature radiation pyrometry on Ti–6Al–4V. *Measurement* **2013**, *46*, 871–880. [CrossRef]

6.   Da Silva, L.J.; Souza, D.M.; De Araújo, D.B.; Reis, R.P.; Scotti, A. Concept and validation of an active cooling technique to mitigate heat accumulation in WAAM. *Int. J. Adv. Manuf. Technol.* **2020**, *107*, 2513–2523. [CrossRef]

7.   Henckell, P.; Günther, K.; Ali, Y.; Bergmann, J.P.; Scholz, J.; Forêt, P. The Influence of Gas Cooling in Context of Wire Arc Additive Manufacturing—A Novel Strategy of Affecting Grain Structure and Size. In *TMS 2017 146th Annual Meeting & Exhibition Supplemental*; Springer: Cham, Germany, 2017; pp. 147–156. [CrossRef]

8.   Cunningham, C.; Dhokia, V.; Shokrani, A.; Newman, S. Effects of in-process LN2 cooling on the microstructure and mechanical properties of type 316L stainless steel produced by wire arc directed energy deposition. *Mater. Lett.* **2021**, *282*, 128707. [CrossRef]

9.   Xu, X.; Ding, J.; Ganguly, S.; Diao, C.; Williams, S. Oxide accumulation effects on wire + arc layer-by-layer additive manufacture process. *J. Mater. Process. Technol.* **2018**, *252*, 739–750. [CrossRef]

10.   Williams, S.W.; Martina, F.; Addison, A.C.; Ding, J.; Pardal, G.; Colegrove, P. Wire + Arc Additive Manufacturing. *Mater. Sci. Technol.* **2016**, *32*, 641–647. [CrossRef]

11.   Lei, Y.; Xiong, J.; Li, R. Effect of inter layer idle time on thermal behavior for multi-layer single-pass thin-walled parts in GMAW-based additive manufacturing. *Int. J. Adv. Manuf. Technol.* **2018**, *96*, 1355–1365. [CrossRef]

12.   Lu, X.; Zhou, Y.F.; Xing, X.L.; Shao, L.Y.; Yang, Q.X.; Gao, S.Y. Open-source wire and arc additive manufacturing system: Formability, microstructures, and mechanical properties. *Int. J. Adv. Manuf. Technol.* **2017**, *93*, 2145–2154. [CrossRef]

13.   Wang, H.; Jiang, W.; Ouyang, J.-H.; Kovacevic, R. Rapid prototyping of 4043 Al-alloy parts by VP-GTAW. *J. Mater. Process. Technol.* **2004**, *148*, 93–102. [CrossRef]

14.   Xiong, J.; Zhang, G.; Qiu, Z.; Li, Y. Vision-sensing and bead width control of a single-bead multi-layer part: Material and energy savings in GMAW-based rapid manufacturing. *J. Clean. Prod.* **2013**, *41*, 82–88. [CrossRef]

15.   Wu, B.; Pan, Z.; Ding, D.; Cuiuri, D.; Li, H.; Fei, Z. The effects of forced interpass cooling on the material properties of wire arc additively manufactured Ti6Al4V alloy. *J. Mater. Process. Technol.* **2018**, *258*, 97–105. [CrossRef]

16.   Ma, C.; Li, C.; Yan, Y.; Liu, Y.; Wu, X.; Li, D.; Han, Y.; Jin, H.; Zhang, F. Investigation of the in-situ gas cooling of carbon steel during wire and arc additive manufacturing. *J. Manuf. Process.* **2021**, *67*, 461–477. [CrossRef]

17.   Scotti, F.M.; Teixeira, F.R.; Da Silva, L.J.; De Araújo, D.B.; Reis, R.P.; Scotti, A. Thermal management in WAAM through the CMT advanced process and an active cooling technique. *J. Manuf. Process.* **2020**, *57*, 23–35. [CrossRef]

18.   Teixeira, F.R.; Scotti, F.M.; Reis, R.P.; Scotti, A. Effect of the CMT advanced process combined with an active cooling technique on macro and microstructural aspects of aluminum WAAM. *Rapid Prototyp. J.* **2021**, *27*, 1206–1219. [CrossRef]

19.   R Rosli, N.A.; Alkahari, M.R.; bin Abdollah, M.F.; Maidin, S.; Ramli, F.R.; Herawan, S.G. Review on effect of heat input for wire arc additive manufacturing process. *J. Mater. Res. Technol.* **2021**, *11*, 2127–2145. [CrossRef]

20.   da Silva, L.; Teixeira, F.; Araújo, D.; Reis, R.; Scotti, A. Work envelope expansion and parametric optimization in WAAM with relative density and surface aspect as quality constraints: The case of Al5Mg thin walls with active cooling. *J. Manuf. Mater. Process.* **2021**, *5*, 40. [CrossRef]

21.   Martina, F.; Mehnen, J.; Williams, S.; Colegrove, P.; Wang, F. Investigation of the benefits of plasma deposition for the additive layer manufacture of Ti–6Al–4V. *J. Mater. Process. Technol.* **2012**, *212*, 1377–1386. [CrossRef]

22.   Ríos, S.; Colegrove, P.; Martina, F.; Williams, S.W. Analytical process model for wire + arc additive manufacturing. *Addit. Manuf.* **2018**, *21*, 651–657. [CrossRef]

23.   Ryan, E.; Sabin, T.; Watts, J.; Whiting, M. The influence of build parameters and wire batch on porosity of wire and arc additive manufactured aluminium alloy 2319. *J. Mater. Process. Technol.* **2018**, *262*, 577–584. [CrossRef]

24.   Da Silva, C.L.M.; Scotti, A. The influence of double pulse on porosity formation in aluminum GMAW. *J. Mater. Process. Technol.* **2006**, *171*, 366–372. [CrossRef]

25.   Toda, H.; Hidaka, T.; Kobayashi, M.; Uesugi, K.; Takeuchi, A.; Horikawa, K. Growth behavior of hydrogen micropores in aluminum alloys during high-temperature exposure. *Acta Mater.* **2009**, *57*, 2277–2290. [CrossRef]

26.   Gu, J.; Ding, J.; Williams, S.W.; Gu, H.; Ma, P.; Zhai, Y. The effect of inter-layer cold working and post-deposition heat treatment on porosity in additively manufactured aluminum alloys. *J. Mater. Process. Technol.* **2016**, *230*, 26–34. [CrossRef]